FACILE CLASSIFICATION OF POLYURETHANE FOAM FROM POST-CONSUMER-USE MATTRESSES

Divya Iyer (divyajayaram@g.ucla.edu) and Samanvaya Srivastava (samsri@ucla.edu)
Chemical and Biomolecular Engineering, University of California, Los Angeles

INTRODUCTION

Mattresses comprise multiple polyurethane (PU) foam layers, metal springs, and textiles. Each foam layer differs in its functionality (e.g., memory foam, support foam), emerging from the variations in the chemical composition of PU foams (e.g., the extent of foaming, cross-linking, nature of backbone, etc.). Current strategies for recycling foams from post-consumer-use mattresses rely primarily on mechanical shredding of foam for subsequent use in carpet underlay. However, the sustainability of this approach is challenged by an expected increase in the supply of post-consumer mattress foam and an expected lower demand for carpet underlay. At the same time, due to a lack of straightforward, field-implementable strategies to segregate these PU foam layers according to their chemical compositions at mattress recycling facilities, avenues for chemical recycling of PU foams from post-consumer-use mattresses remain limited.

This work proposes a simple rebound test to classify post-consumer-use mattress foam. By investigating the physico-mechanical and thermo-chemical properties of over 110 foam layers collected from 60 post-consumer-use mattresses of different ages manufactured globally, a correlation was established between the observed physical properties (e.g., rebound resilience) and chemical composition (degree of cross-linking, nature of polyol) of these layers. Therefore, we show that a simple ball rebound test can offer valuable insights into the chemical composition and facilitate easy classification (e.g., conventional or viscoelastic foams) to ensure a cleaner feedstock for alternative recycling solutions. Additionally, this correlation between the physical and thermo-chemical properties can aid the development of recycling strategies tailored to each type of foam based on the nature of the backbone, the extent of cross-linking, and thermal stability. Finally, analytical characterization did not detect chemical traces of PFAS or 2-ethyl hexanoic acid.

BACKGROUND

Polyurethanes (PU) are produced by the reaction between a polyol (OH) and a diisocyanate (NCO) group (**Scheme 1A**). The type of PU (e.g., foam, dispersion, elastomer) depends on the chemical composition (e.g., isocyanate index, type of diisocyanate and polyol) and series of reactions (e.g., cross-linking, foaming, etc.). In the synthesis of flexible PU foam, the cross-linking (**Scheme 1A**) and foaming reactions (**Scheme 1B**) occur synchronously. The relative extent of the two reactions depends primarily on the type of polyol being used and the isocyanate index (NCO : OH). The reactivity of isocyanate groups to multiple OH-containing species and water renders PU foam compositions tunable. For example, in addition to the PU network formation (cross-linking), the reaction of isocyanate groups with water is an essential step in the synthesis of PU foam. Reactive isocyanate groups form an unstable intermediate (carbamic acid) upon reaction with water, eventually releasing carbon dioxide and forming amines **(Scheme 1B)**; the carbon dioxide formation leads to the porous nature of foams. The amine groups can further react with excess isocyanate to form urea linkages in addition to the primary PU network. Therefore, to attain a greater extent of foaming, a high isocyanate index (NCO : OH > 1) is preferred, while a low isocyanate index (NCO : OH < 1) or the use of a high OH-

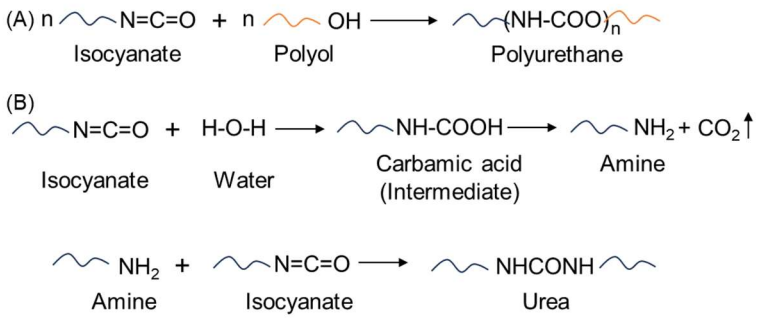

Scheme 1: (A) Formation of urethane linkages by reaction of an isocyanate with polyol (B) Reaction of isocyanate with water eventually forms an amine and carbon dioxide. The amine reacts with isocyanate to form urea linkages.

value polyol lead to a larger extent of the crosslinking reaction.[1,2] The relative extent of these two reactions (crosslinking vs. foaming) and the type of bonds in the network dictate the foam structure and PU foam properties (e.g., density, shock absorption ability).

Prior studies have indicated that the fabrication of viscoelastic (memory) PU foam involves the use of low molecular weight (M_w 700 – 2000 g/mol) polyols (high OH-value), leading to a more cross-linked (urethane linkages) network as compared to conventional foams (M_w> 3000 g/mol).[3] Additionally, low isocyanate indices (NCO : OH = 0.5 – 1.05) and lower water contents (0.75 – 2.5 parts per hundred polyol; php) are preferred for viscoelastic foam synthesis to minimize foaming. In contrast, high isocyanate indices (NCO : OH > 1.05) and higher water contents (3 – 5 php) are preferred for fabricating conventional foams to produce more urea linkages and foaming.[1–3] Properties such as density, foam cell structure, and shock absorption are controlled by altering the chemical composition, thus making them suitable for different applications (e.g., furniture, memory foam mattresses, shoes, etc.). However, when these PU foams are disposed of post-use, the lack of practical and facile strategies to identify these differences in chemical composition hinders their recycling. Here, we correlate the complex chemical composition of post-consumer-use PU foam layers to physical properties that can be observed and quantified to facilitate the development of field-implementable foam classification strategies.

Results and Discussion

Mattress Foam Statistics.

The post-consumer-use mattress layers characterized in this study were procured from a Los Angeles, CA-based mattress recycler. 111 sample layers were collected from 60 all-foam and innerspring mattresses. Of all the samples collected, 87% originated from all-foam mattresses, while the rest were obtained from innerspring mattress layers (**Figures 1A and 1B**). The studied sample set predominantly consisted of all-foam mattresses due to challenges associated with procuring samples of the recommended dimensions (the thickness was lesser than the recommended 2 inches) for the rebound resilience test.

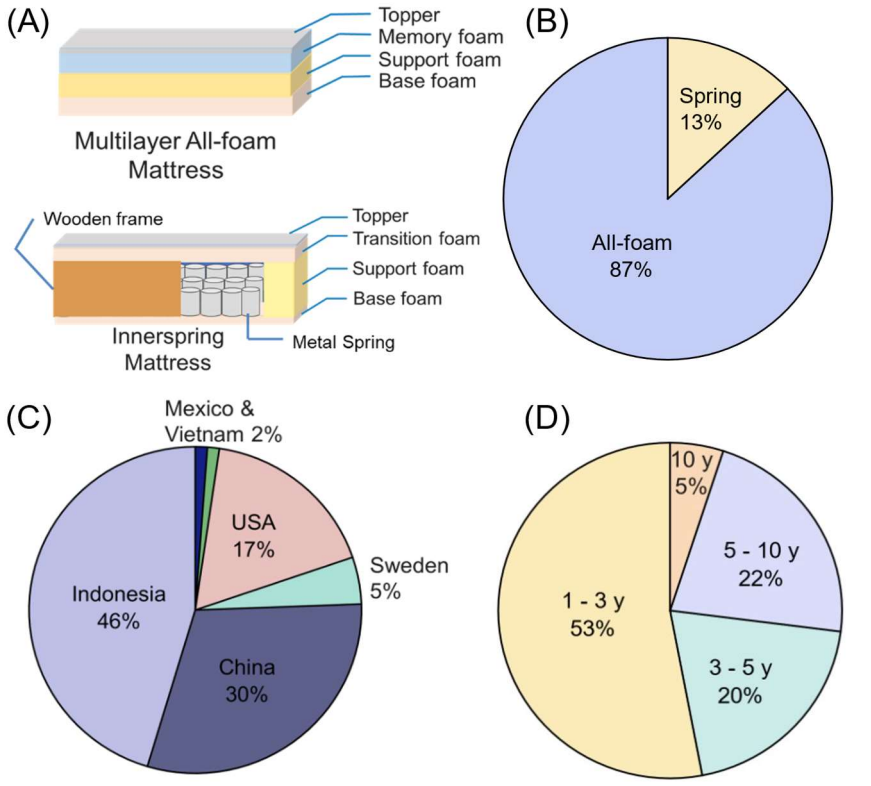

Figure 1: (A) Samples were collected from all foam mattresses and innerspring mattresses (support foam layer). Distribution of layers based on (B) type, (C) country of origin, and (D) age. Sample sizes were 111 layers for (B) and 89 layers for (C, D).

The country of origin and age tags were available for 33 mattresses (comprising 89 foam layers). Although all mattresses were procured from an MRF in California, interestingly, most of these mattresses were manufactured outside the United States, predominantly in Indonesia and China (**Figure 1C**). The age of the foam layers ranged between 1 and 10 years, with a majority being 1 to 3 years old (**Figure 1D**). Within the subset of innerspring mattress layers, tags were available for ~33% of the layers; a trend similar to the all-foam mattresses was observed wherein the layers were between 3–7 years old and were predominantly manufactured outside the United States (Sweden, Mexico). Specific efforts were made to maximize the proportion of tagged mattresses in this study; untagged mattresses (for which manufacturing date and location information is unavailable) may likely be older.

Rebound Resilience: The Basis for Foam Classification.

The ball-rebound values formed the basis for classifying the 111 foam layers collected from 60 mattresses. The Polyurethane Foam Association (PFA) provides the ranges for the classification of PU foam based on the rebound values; viscoelastic foams typically have a low rebound value (< 20%), while other flexible foam types (e.g., conventional) have higher rebound values.[4] As shown in **Figure 2A**, a clear segregation in the ball-rebound values was observed for the post-consumer-use mattress foam layers. Of the 111 foam layers, nearly 75% (83 samples) possessed rebound resilience values > 27% and were classified as conventional foams. The remaining 25% had low rebound values (< 12%) and were categorized as viscoelastic foams. Since a clear distinction in rebound resilience was noted, this test formed the basis for the classification of foams. Interestingly, all the samples from innerspring mattresses were conventional foams (rebound resilience > 27%), while the multilayer mattresses comprised a combination of both kinds of foams. No intermediate values of rebound resilience were observed for the foams.

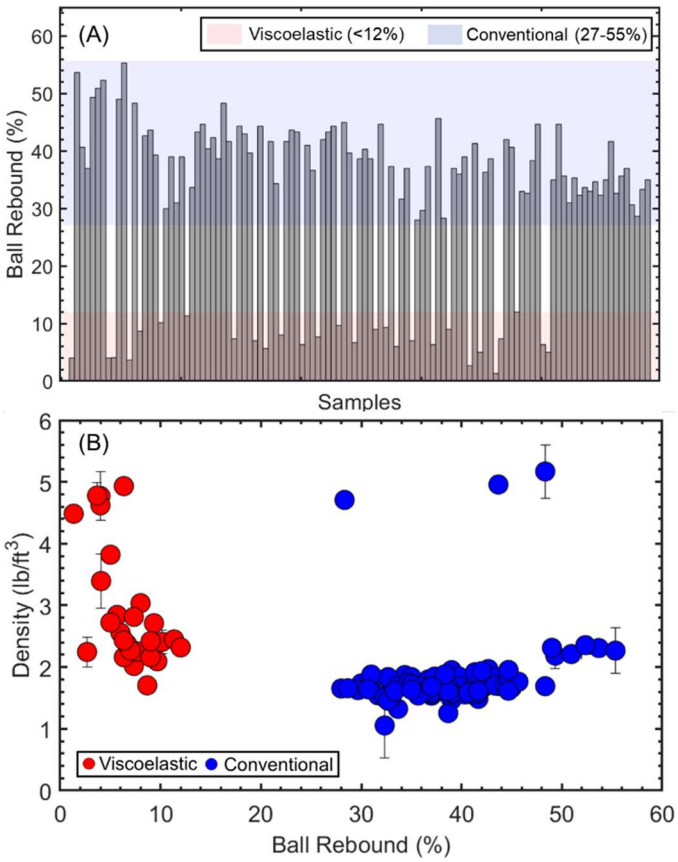

Figure 2: (A) The ball rebound (resilience) values (%) of 111 mattress foam layers classified as viscoelastic and conventional foams. (B) The measured density of mattress foam layers as a function of ball rebound.

Since a precise categorization in rebound resilience values was noted, they were used to compare the physico-mechanical (density, compression) and thermo-chemical (composition, T_g) attributes of the foams. For instance, the density of viscoelastic foams ranged from 1.5 lb/ft^3 to 5 lb/ft^3, while the conventional foams had lower densities (1–2.2 lb/ft^3) (**Figure 2B**). Although a distinction in density between the two categories (viscoelastic and conventional) was not observed owing to the overlap in density ranges, the density variation within the conventional foams was minimal (**Figure 2B**).

A quadrant analysis investigating the distribution of the rebound resilience and density values (**Figure 3**) of viscoelastic foams (**Figure 3A**) and conventional foams (**Figure 3B**) confirmed the minimal variation of the density of conventional foams around the mean (1.84 lb/ft^3) (**Figure 3B**) as compared to the viscoelastic foams (2.9 lb/ft^3) (**Figure 3A**). Higher density values corresponded with lower resilience within the viscoelastic foam category (**Figure**

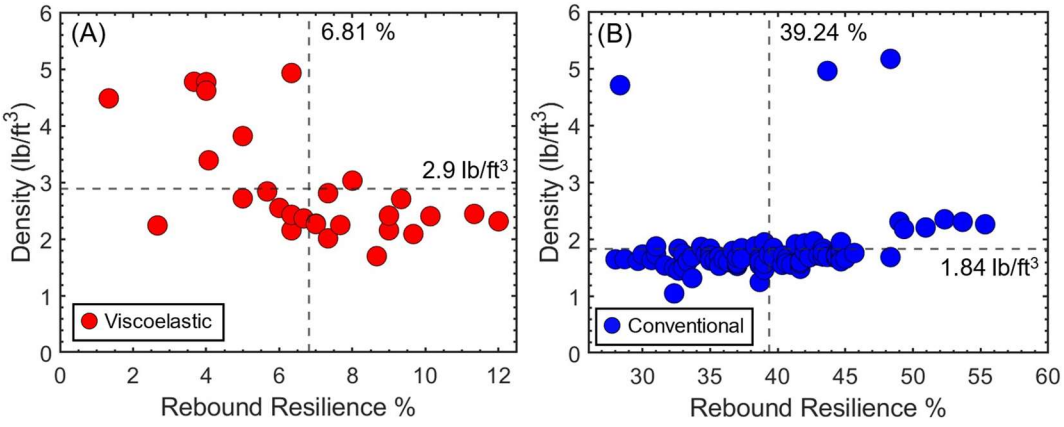

Figure 3: A quadrant analysis of the density and rebound resilience values of (A) viscoelastic foams and (B) conventional foams representing the distribution around the mean values.

3A). Additionally, this analysis revealed outliers in the conventional foam samples with resilience values within the range prescribed for conventional foams (27–55%) but with density values significantly higher than the population mean. Interestingly, conventional foams with resilience values higher than ~50% possessed density values that deviated slightly from the population mean but cannot be deemed as outliers (**Figure 3B**).

The Compressive Resistance and Resilience of PU Foams are Interdependent.

Compressive resistance and resilience of the foams were evaluated for 45 samples by performing cyclic compression-decompression tests. Examples of stress-strain curves are shown in **Figure 4A**. From such stress responses, the resistance to deformation (maximum stress; **Figure 4B**) and the compression modulus (**Figure 4C**) were calculated for all the samples. These parameters are shown as a function of the rebound resilience values in **Figures 4B** and **4C**. The deformation resistance was lower for viscoelastic foams (< 0.02 MPa), while conventional foams had resistance values spread over a wide range (0.002 MPa – 0.045 MPa; **Figure 4B**). A similar distinction between the viscoelastic and conventional foams was also made based on the compressive moduli (**Figure 4C**). The viscoelastic foams' low rebound resilience values strongly indicate their highly damping nature (slower recovery from stress). The damping ratio determined from the stress-strain curves did not exhibit correlations with the rebound resilience values; we attribute this divergence to the low strain rates (1 mm/min) at which the compression resistance characterization was performed, as opposed to the rebound resilience tests which are instantaneous. We, therefore, posit that the rebound resilience is a good indicator of the difference in damping properties between the viscoelastic and conventional

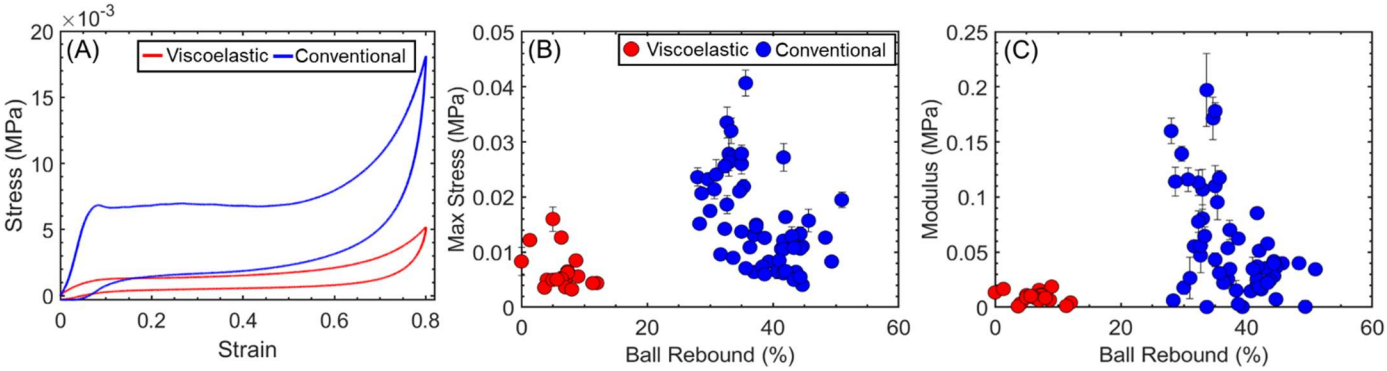

Figure 4: (A) Representative stress-strain curves. Similar curves were obtained for 45 foam samples. The (B) maximum stress (indicating resistance to deformation), and (C) the compression modulus of those foam layers were calculated as a function of rebound resilience values.

foams, while the differences in deformation resistance (**Figure 4B**) and compression moduli (**Figure 4C**) can be determined by compression-decompression tests.

Under compression, the foam cell structure is strained, followed by failure and densification.[5] The low moduli and low resistance of viscoelastic foams indicate the ability of the viscoelastic foam structures to sustain high strains without a stress buildup. This can be attributed to the low porosity of the viscoelastic foams, as shown in the scanning electron microscopy (SEM) images (**Figures 5A and 5B**), in addition to their densely cross-linked structure (discussed in the next section). In contrast, conventional foams have a more porous cell structure (**Figures 5C and 5D**), corresponding to a greater extent of cell opening and a lower extent of urethane formation, as discussed later. These characteristics led to larger resistance to deformation

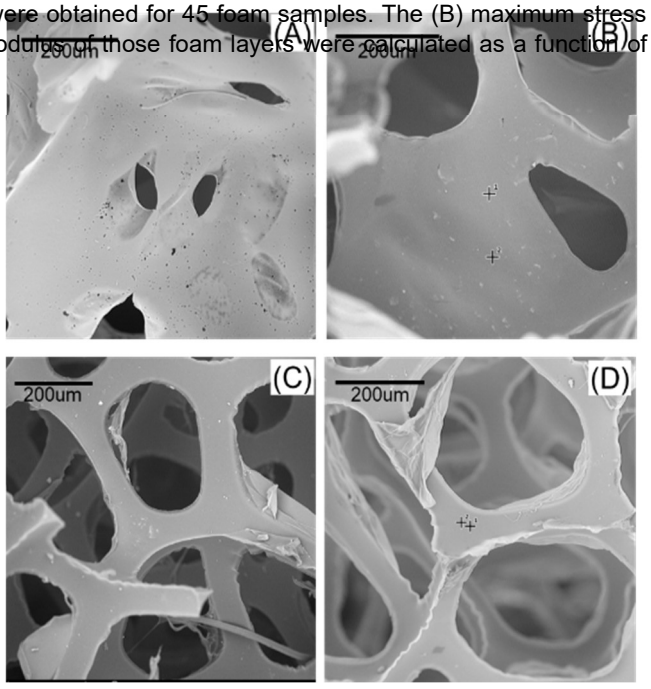

Figure 5: SEM images of representative (A – B) viscoelastic and (C – D) conventional foam layers.

and moduli values for conventional foams. We note that the differences in porosity also concur with the differences in rebound resilience between the two categories of foams. Moreover, the non-uniformities in the foam cell structure and susceptibility to cell collapse upon deformation in conventional foams may also result in significant variation in their compressive properties, as is evident in **Figures 4B and 4C**.

Foam Composition and Thermo-Chemical Properties Correlated Strongly with Rebound Resilience.

The chemical composition of 65 viscoelastic and conventional foams was assessed by Fourier-transform infrared (FTIR) spectroscopy in the wavenumber range of 500 – 2000 cm^{-1}. The spectra for both types of foams predominantly comprised similar peaks corresponding to the polyurethane backbone (**Figure 6A**), including C–O–C (ether, 1180 cm^{-1}), N–H (amide/amine, 1520 cm^{-1}), CH_2 (methylene, 1380 cm^{-1}), and C=O (bidentate H-bonded urea 1640 cm^{-1} and free urethane 1725 cm^{-1}). However, there were notable differences in the appearance and the relative intensity of some peaks. For example, peak splitting is observed in the N–H peak (1520 cm^{-1}) for the viscoelastic foams, as opposed to a single peak in the conventional foam spectra (**Figure 6A**). This split peak in viscoelastic foams may be attributed to the presence of N–H bond in urethane, unreacted amine (due to low isocyanate index) (**Scheme 1B**), and minor urea peaks, as opposed to the dominant N–H (urea) peak in conventional foams.

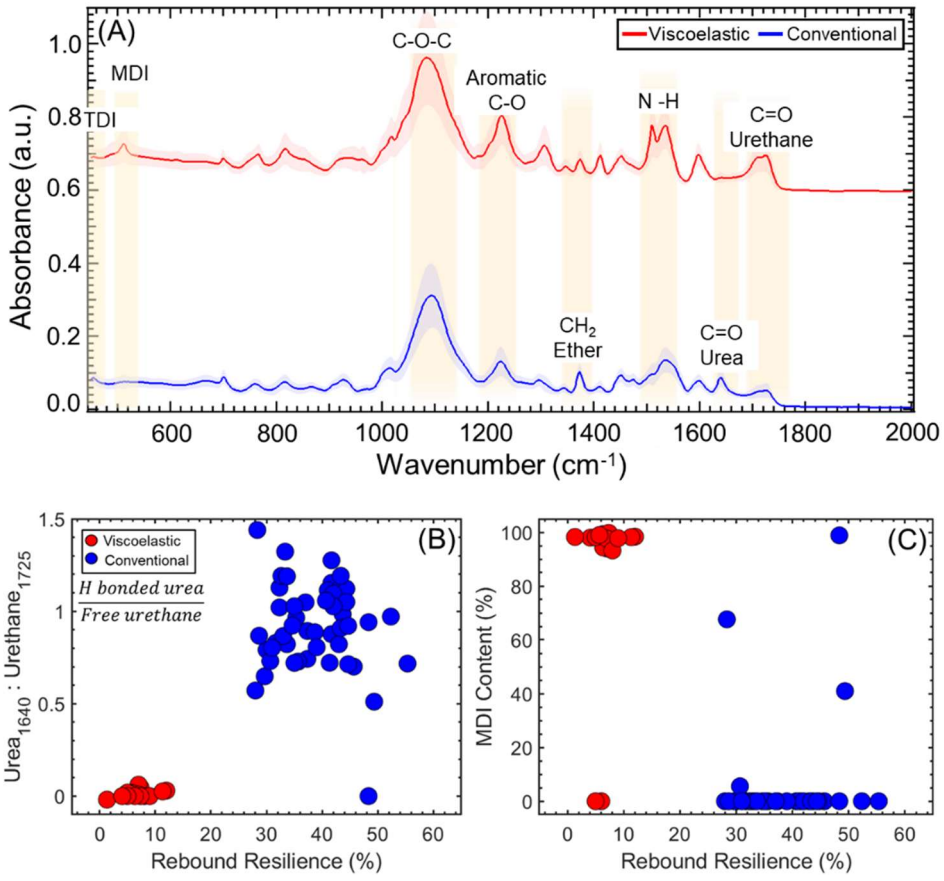

Figure 6 (A) FTIR spectra of viscoelastic and conventional foams were obtained. Ratios of absorbances of the **(B)** bidentate H-bonded urea and free urethane, and **(C)** MDI content were obtained from the FTIR spectra for both categories of foams.

Interestingly, the bidentate H-bonded urea peak (1640 cm^{-1}) was more evident than the urethane peak (1725 cm^{-1}) in the FTIR spectra for conventional foams, while the urethane peaks were more dominant as compared to the bidentate H-bonded urea peaks in the spectra for the viscoelastic foams (**Figure 6A**). Correspondingly, the viscoelastic foams were found to have lower urea/urethane (< 0.5) values as compared to conventional foams (> 0.5) (**Figure 6B**). Simultaneously, a strong correlation between these values and the ball rebound values was noted for both types of foams (**Figure 6B**). The low values of urea/urethane reveal a lower extent of urea formation in viscoelastic foams than in conventional foams (**Scheme 1**). Concomitantly, it is evident that the extent of the urethane formation reaction dominates over the urea formation reaction and open cell formation in viscoelastic foams. A greater extent of bidentate urea linkage indicates hard and soft segment phase segregation and consequent open cell structure formation, consistent with observations of the foam structures under an electron microscope (**Figure 5**) and with foam synthesis compositions from prior studies.[1–3,6–8] Typically, higher water contents are used to synthesize

conventional PU foams (compared to viscoelastic foams) to initiate foaming (urea formation) reactions and consequent formation of an open cell structure, also leading to their overall lower densities (**Figure 2B**).[1,2]

Furthermore, FTIR analysis was used to identify the diisocyanate used in the viscoelastic and conventional foam layers (**Figure 6C**). The TDI and MDI peaks were identified at 454 cm^{-1} and 510 cm^{-1}, respectively, from the FTIR spectra (**Figure 6A**). Since the concentration of each functional group is proportional to the absorbance values,[9] the relative ratios of the peak heights were quantified to determine the relative concentration of each diisocyanate (**Figure 6C**). We note that these values represent the relative proportions of MDI and TDI in the foam samples, not the absolute concentrations of the diisocyanates. Of the conventional foams characterized by FTIR (49 samples), 94% (46 samples) were identified to be 100% TDI-based, while a small proportion of the samples were obvious outliers (**Figure 6C**). In the viscoelastic foam sample set (16 samples), 2 samples were obvious outliers, while the rest were identified to have an MDI content of 94–100 % (**Figure 6C**). This distribution of MDI contents in the viscoelastic samples can be attributed to minor errors owing to the inherently weak nature of the MDI and TDI peaks in the spectra (**Figure 6A**).

This distinction between the chemical composition of viscoelastic and conventional foam layers is further corroborated by the differences in their glass transition temperatures (T_g) determined from differential scanning calorimetry (DSC) (**Figure 7A**). Overall, higher T_g values were noted for viscoelastic foams than for conventional foams (**Figure 7B**). These higher T_g values for viscoelastic foams can be attributed to higher cross-linking density arising from the use of high-OH value polyols, leading to hindered molecular rearrangement.[3] These observations are underscored by the slow recovery, superior shock-absorbing behavior, and damping (low rebound resilience, **Figure 2B**) of viscoelastic foams compared to conventional foams. It has been suggested that viscoelastic foams can possess widely varying T_g values, even as high as 35 – 40 °C, depending on the OH-value and MW of the polyol.[10] These higher T_g values render them suitable as memory foam layers in mattresses. The lower T_g values for conventional foams can be ascribed to the lower extent of cross-linking (**Figure 6A**), thus facilitating rearrangements and relaxation, leading to a higher rebound resilience.

To understand the influence of the extent of cross-linking and foaming on the thermal stability of these foam layers, thermogravimetric analyses (TGA) were performed on representative samples (**Figure A2**). No significant weight loss (< 1 – 2%) was observed at temperatures less than 250 °C. The degradation temperatures (corresponding to the most significant weight loss) for both types of foams ranged between 400 – 450 °C and did not reveal any significant differences between the two categories, despite the onset of degradation occurring at a higher temperature for the viscoelastic foams. (**Figure A2**). Interestingly, despite no differences in thermal stability, the findings from FT-IR spectroscopy and DSC enable the distinction between the two types of foam.

Evidence of Tin Derivatives and Halogens Noted in Post-Consumer-Use Foams

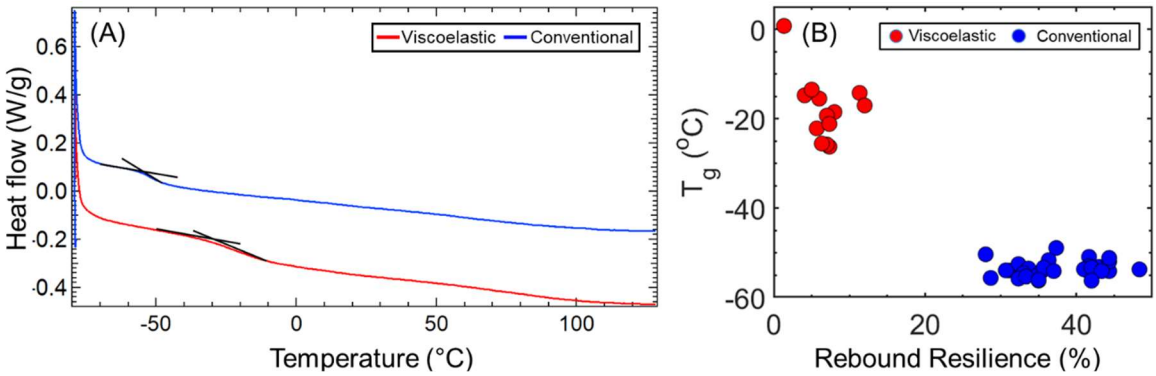

Figure 7 (A) DSC curves for viscoelastic and conventional foam layers were used to calculate the **(B)** T_g values for viscoelastic and conventional foam layers as a function of rebound resilience.

The viscoelastic and conventional foams predominantly comprised carbon (C), nitrogen (N), and oxygen (O) attributed to the polyurethane backbone (**Table 1**; values represent the mean of triplicate measurements along with standard error). Additionally, specific efforts using X-ray fluorescence (XRF) spectroscopy were made to detect and quantify elements such as tin (Sn) and bismuth (Bi) (often originating from organometallic catalysts used in PU foam manufacturing), as well as halogens (Cl, Br, F) typically used in flame retardants. While the concentration of Sn ranged between ~ 2–160 ppm (6.9 – 551.72 ppm stannous octoate), Bi was present in much lower concentrations (0.4–1.7 ppm). Stannous octoate – one of the most commonly employed organometallic catalysts – is generally added at 0.05 – 0.5 wt% (i.e., 1000 ppm) in combination with other organic (e.g., amine catalysts).[11,12] The lower concentrations of Sn could be indicative of greater proportions of other organic catalysts.

	Conventional			Viscoelastic		
	Sample 1	Sample 2	Sample 3	Sample 1	Sample 2	Sample 3
	Indonesia, 2021	No tag available	No tag available	Indonesia, 2021	Indonesia, 2021	China, 2015
C (wt%)	61.66 ± 1.68	63 ± 1.37	65.37 ± 1.27	62.18 ± 1.33	59.6 ± 1.55	56.32 ± 1.57
N (wt%)	10.27 ± 0.77	11.05 ± 1.14	12.54 ± 0.98	6.16 ± 0.49	6.89 ± 0.52	11.88 ± 0.83
O (wt%)	29.75 ± 1.85	29.24 ± 1.91	25.6 ± 1.16	34 ± 1.11	34.8 ± 1.84	34.89 ± 2.4
Sn (ppm)	158 ± 8.72	128.5 ± 2.41	138.78 ± 12.21	6.15 ± 1.18	2.37 ± 2.37	15.19 ± 0.91
Cl (ppm)	2489.5 ± 226.26	109.55 ± 6.29	111.17 ± 20.05	4175 ± 290	438 ± 22.12	3240 ± 104.7
Br (ppm)	1.7 ± 0.9	2.07 ± 0.6	2.07	5.12	6.09 ± 1.01	0.35 ± 0.35
F (ppm)	0	7.24 ± 7.24	0	0	0	0
Bi (ppm)	0	1.72 ± 0.91	0	1.71 ± 0.9	1.10 ± 1.10	0.69 ± 0.35

Table 1: Composition of representative conventional foams and viscoelastic foams as determined by X-ray fluorescence (XRF) measurements.

The presence of halogenated compounds – predominantly Cl (and Br) – likely indicates the presence of halogenated flame retardants (e.g., tris-2-chloro-ethyl phosphate, polybrominated diphenyl ethers).[13] Notably, the use of these halogenated flame retardants in sold/distributed products has been banned in several states in the US (beyond 1000 ppm) since 2020.[13] Yet, while the concentration of Br was well below the acceptable limits, Cl was detected in high concentrations in some of the samples.

No Traces of PFAS Noted in Post-Consumer-Use Foams.

PFAS, also known as 'forever chemicals,' are resistant to most remedial processes and can impede material recycling. PFAS (PF-butanoic acid, PF-hexanoic acid, PF-octanoic acid, and PF-octane sulfonic acid) were not detected in representative conventional and viscoelastic foam samples (two samples each of viscoelastic and conventional foams were tested).

2-Ethyl Hexanoic Acid Not Detected in Mattress Foams.

2-ethyl hexanoic acid (used as a catalyst – in the salt form, as well as generated on the degradation of stannous octoate) was not detected by thermogravimetric analysis (TGA) - mass spectrometry (MS) in representative viscoelastic and conventional foam samples (6 samples; 3 from each category) (**Figure 8A** and **Figure A3-A7**). The most evident peak was noted at 28 atomic mass units (amu; from nitrogen, which was employed as the purge gas). Peaks of significantly lower intensity were also observed at 14 amu (ionized moiety from the purge gas), 27 amu, and 29 amu. The ion current measurements at 27 amu and 29 amu are congruent to the reference spectrum for 2-ethyl hexanoic acid (**Figure 8B**). However, since they remain constant over time (even as the TGA progresses) (**Figure 8A, *Inset***), they are most likely secondary peaks from the purge gas. Additionally, when compared with the reference spectrum for 2-ethyl hexanoic acid (**Figure 8B**),[14] the base peaks (highest intensity) expected at 88 amu (followed by 73 amu and 41 amu) are absent (**Figure 8A** and **Figure** 8**A, *Inset***) in the spectrum, thereby confirming that 2-ethyl hexanoic acid was not detected.

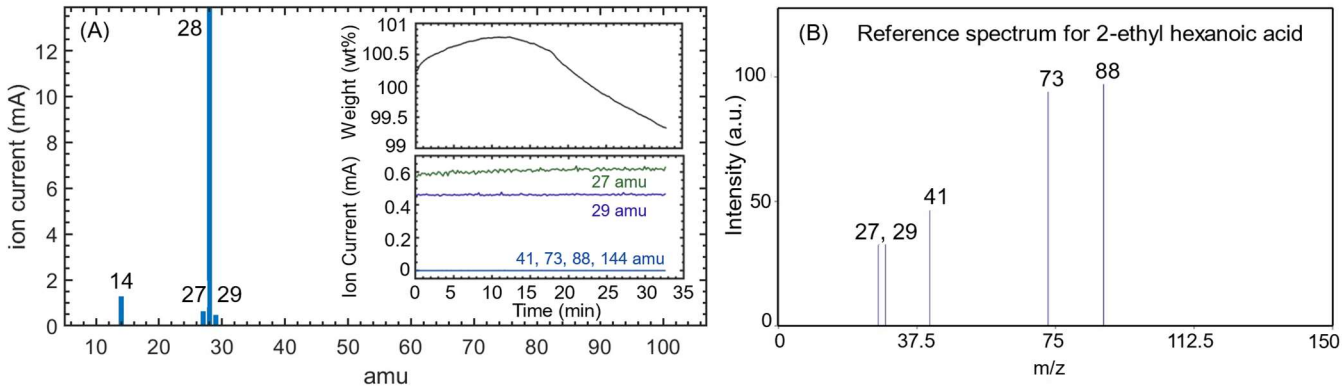

Figure 8: Mass spectrum of **(A)** evolved gases from a representative mattress sample. *Inset*: The time evolution of the weight of the heated foam upon heating (top panel) and the ion current corresponding to the peaks at 27, 29, 41, 73, 88, and 144 amu (bottom panel). **(B)** Reference mass spectrum of 2-ethyl hexanoic acid.

Discarded Mattresses are Inhabited by Bacteria and Mold.

Seven representative foam samples were evaluated (3 viscoelastic samples and 4 conventional samples) and all exhibited the potential to proliferate into bacterial and mold colonies (**Figure 9**). As compared to the negative control (agar plate) (**Figure 9A, C**), the plates in contact with the foam samples exhibited a significant growth of bacterial (post overnight incubation at 37 °C; representative sample **Figure 9B** and other samples shown in **Figure A8**) and mold colonies (incubated at room temperature for 6 days; representative sample shown in **Figure 9D,** and other samples shown in **Figure A9**). The bacterial (**Figure 9E**) and mold (**Figure 9F**) colonies were quantified and compared with typical values for indoor air (black bars in **Figure 9E, F**).[15,16] Although only a limited number of samples were evaluated, the results indicate that discarded mattresses exhibit the potential to result in microbial growth and

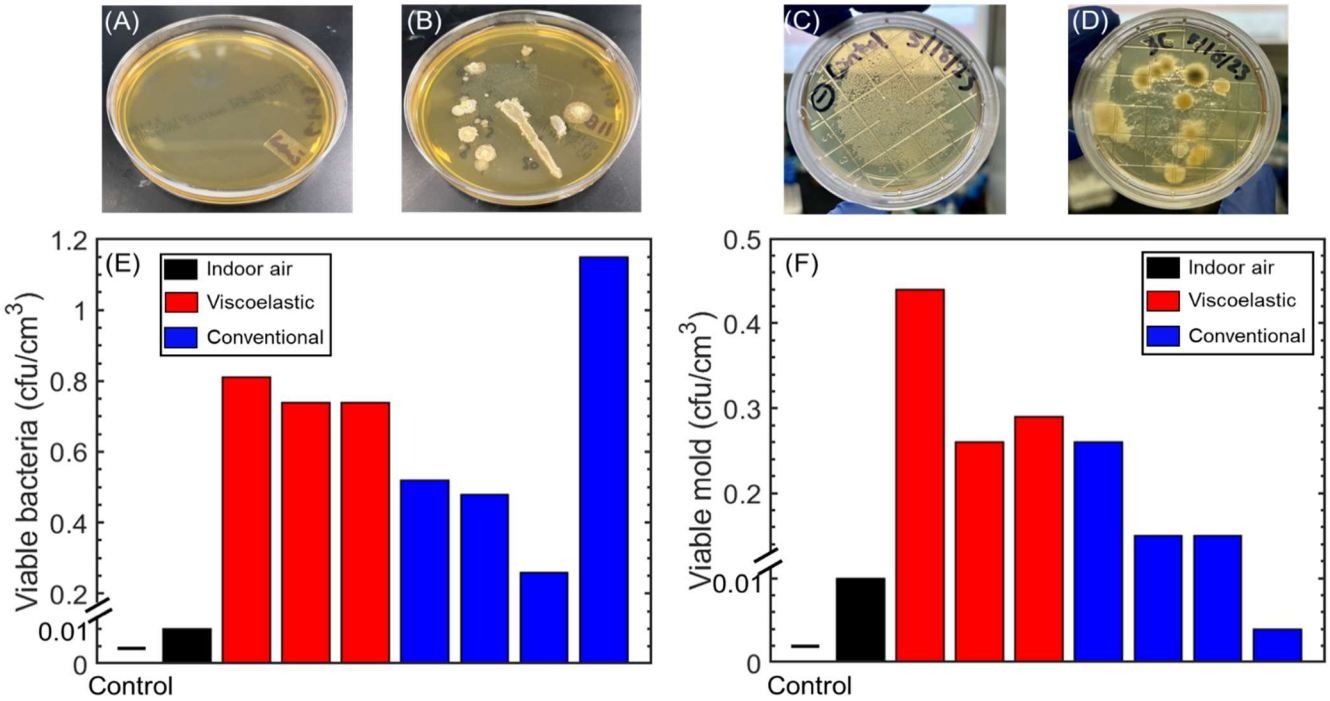

Figure 9: Images of agar plates with **(A)** negative control and **(B)** bacterial colonies from a representative mattress sample, and **(C)** negative control and **(D)** mold colonies from a representative mattress sample. The viable **(E)** bacterial and **(F)** mold colonies for viscoelastic and conventional samples were quantified and compared with the negative control (no growth observed) and reference values for indoor air.

proliferation, presumably due to exposure to moisture and dampness over the course of their use at temperatures conducive to bacterial and mold growth (68 – 80 °F).

CONCLUSIONS

This report proposes a strategy to classify foams from post-consumer-use mattresses. Over 110 samples were collected from 60 mattresses of different ages manufactured globally. By systematically characterizing the physical (rebound resilience, density), mechanical (behavior under compression), and thermo-chemical (nature of backbone and T_g of these layers, it is posited that the rebound resilience could form the basis for the classification of these foams. The simple ball-rebound test can aid the classification of foams into viscoelastic (resilience < 15%) and conventional (resilience > 27%) foams. While the conventional foams possessed markedly lower densities, the viscoelastic foams had a wide variation in density. Additionally, viscoelastic foams exhibited higher damping (lower rebound resilience), lower deformation resistance and compression moduli, while conventional foams exhibited larger variations in compression resistance. Similar to the distinction observed with the ball rebound values, quantifying the chemical composition from FTIR offered valuable insights. The viscoelastic foams had lower urea : urethane ratio as compared to the conventional foams, indicating a lower extent of the foaming (urea formation) and cell opening reactions but a greater extent of cross-linking (urethane formation) in viscoelastic foams. Additionally, viscoelastic foams were identified to be predominantly MDI-based, while conventional foams are TDI-based. The DSC analysis indicated higher T_g values for the viscoelastic foams than for the conventional foams, thus confirming the former's highly branched and cross-linked nature compared to the latter. Finally, analytical characterization revealed that PFAS and 2-ethyl hexanoic acid were not detected in representative samples of post-consumer-use mattresses, while tin (catalyst; 2 – 160 ppm) and halogens (Cl 109 – 4000 ppm; Br 0.35 – 6 ppm) were detected in ppm-scale amounts. Tests to detect bacteria and mold growth confirmed that discarded foam samples exhibit potential for microbial growth and proliferation. Thorough physico-mechanical and thermo-chemical characterization of these foams presents rebound resilience as a well-defined and field-implementable strategy that correlates to information about the composition of post-consumer-use foam layers. Additionally, the rebound resilience values (correlated with the extent of cross-linking and degree of polyol branching) can facilitate the development of recycling strategies tailored to each type of foam.

ACKNOWLEDGMENTS

We thank Dr. Sanjay Mohanty (UCLA), Dr. Lihua Jin (UCLA), and Dr. John Hayes (Covestro) for their support and constructive discussions. The DSC, TGA-MS, and XRF measurements were done at the Materials Research Laboratory (UCSB), and we thank Dr. Rachel Behrens, Dr. Amanda Strom, Cesar Rodriguez, Dr. Miguel Zepeda-Rosales, and Dr. Youli Li for their support. We are grateful to Mark Patti (MRC) and Luis Ponce and his team (Cristal Materials) for their support in procuring the samples.

REFERENCES

(1) Aou, K.; Schrock, A. K.; Ginzburg, V. V.; Price, P. C. Characterization of Polyurethane Hard Segment Length Distribution Using Soft Hydrolysis/MALDI and Monte Carlo Simulation. *Polymer (Guildf).* **2013**, *54* (18), 5005–5015. https://doi.org/10.1016/j.polymer.2013.07.014.

(2) Lefebvre, J.; Bastin, B.; Le Bras, M.; Duquesne, S.; Paleja, R.; Delobel, R. Thermal Stability and Fire Properties of Conventional Flexible Polyurethane Foam Formulations. *Polym. Degrad. Stab.* **2005**, *88* (1), 28–34. https://doi.org/10.1016/j.polymdegradstab.2004.01.025.

(3) Moreno, M. R.; Gonzalez, F. J. C.; Fernandez, S. S.; Ramos, E. D. Method for Sorting Flexible Polyurethane Foams. WO 2022/263664 A1, 2022.

(4) Association, P. F. Viscoelastic (Memory) Foam. *InTouch* **2016**, *11*, 1–7.

(5) Mane, J. V.; Chandra, S.; Sharma, S.; Ali, H.; Chavan, V. M.; Manjunath, B. S.; Patel, R. J. Mechanical Property Evaluation of Polyurethane Foam under Quasi-Static and Dynamic Strain Rates- An Experimental Study. *Procedia Eng.* **2017**, *173*, 726–731. https://doi.org/10.1016/j.proeng.2016.12.160.

(6) De Haseth, J. A.; Andrews, J. E.; McClusky, J. V.; Priester, R. D.; Harthcock, M. A.; Davis, B. L. Characterization of Polyurethane Foams by Mid-Infrared Fiber/FT-IR Spectrometry. *Appl. Spectrosc.* **1993**, *47* (2), 173–179. https://doi.org/10.1366/0003702934048334.

(7) Zhao, W.; Nolan, B.; Bermudez, H.; Hsu, S. L.; Choudhary, U.; van Walsem, J. Spectroscopic Study of the Morphology Development of Closed-Cell Polyurethane Foam Using Bio-Based Malonic Acid as Chain Extender. *Polymer (Guildf).* **2020**, *193*, 122344. https://doi.org/10.1016/j.polymer.2020.122344.

(8) El Hatka, H.; Hafidi, Y.; Ittobane, N. Exploring Urea Hard Segment Morphology and Phase Separation Behavior in Flexible Polyurethane Foam Formulations: Water, Lithium Chloride and Isocyanate Structure Effects. *Polym. Polym. Compos.* **2023**, *31*, 1–10. https://doi.org/10.1177/09673911231196380.

(9) Donaldson, P. M. Spectrophotometric Concentration Analysis Without Molar Absorption Coefficients by Two-Dimensional-Infrared and Fourier Transform Infrared Spectroscopy. *Anal. Chem.* **2022**, *94* (51), 17988–17999. https://doi.org/10.1021/acs.analchem.2c04287.

(10) Lutter, H.-D.; Neff, A. R.; Gummaraju, R.; Smiecinski, M. T. Viscoelastic Polyurethane Foam. WO 2005/003206 A1, 2005.

(11) Kiss, G.; Rusu, G.; Bandur, G.; Hulka, I.; Romecki, D.; Péter, F. Advances in Low-Density Flexible Polyurethane Foams by Optimized Incorporation of High Amount of Recycled Polyol. *Polymers (Basel).* **2021**, *13* (11), 1–15. https://doi.org/10.3390/polym13111736.

(12) El Khezraji, S.; Thakur, S.; Raihane, M.; López-Manchado, M. A.; Belachemi, L.; Verdejo, R.; Lahcini, M. Use of Novel Non-Toxic Bismuth Catalyst for the Preparation of Flexible Polyurethane Foam. *Polymers (Basel).* **2021**, *13* (24). https://doi.org/10.3390/polym13244460.

(13) Kalmes, R.; Lee, D.; Robrock, K.; Worthen, A. Massachusetts Latest to Ban Certain Flame Retardants in Selected Consumer Products https://www.exponent.com/article/massachusetts-latest-ban-certain-flame-retardants-selected-consumer-products#:~:text=Only some flame retardants (e.g.,any product by selected states. (accessed Jan 9, 2024).

(14) National Library of Medicine. Compound Summary: 2-Ethyl Hexanoic Acid.

(15) Wanner, H.-U.; Verhoff, A.; Colombi, A.; Flannigan, B.; Gravesen, S.; Mouilleseaux, A.; Nevalainen, A.; Papadakis, J.; Seidel, K. *Biological Particles in Indoor Environments*; 1993.

(16) Rao, C. Y.; Burge, H. A.; Chang, J. C. S. Review of Quantitative Standards and Guidelines for Fungi in Indoor Air. *J. Air Waste Manag. Assoc.* **1996**, *46* (9), 899–908. https://doi.org/10.1080/10473289.1996.10467526.

(17) Kung'u, J. Taking Air Samples For Mold Testing: Settle Plate Method https://www.moldbacteriaconsulting.com/fungi/taking-air-samples-for-mold-testing.html#:~:text=Settle Plates Results,(CFUs) per unit time (accessed Jun 23, 2023).

APPENDIX

Materials & Methods

PU foam layers (111 samples) from 60 post-consumer multilayer mattresses were collected from a mattress recycling facility in the Los Angeles, CA area. Individual layers were obtained by manually separating them from the mattress, and each layer was cut to specific dimensions using Proxxon 37080 Hot Wire Cutter Thermocut 115/E.

Physico-Mechanical Properties

The rebound resilience of each layer was determined by performing the ball rebound test on foam samples with dimensions 100 mm × 100 mm × 50 mm. A steel ball (Φ = 10mm) was released from the top of a transparent polycarbonate tube (Φ = 50 mm, 500 mm length) onto a foam sample placed beneath the tube, and the height of the ball rebound was recorded. The rebound value was estimated as:

$$Ball\ Rebound\ (\%) = \frac{Rebound\ Height}{Initial\ Height} \times 100$$

Post rebound resilience measurements, 3 samples of each layer of dimensions 30 mm × 30 mm × 30 mm were weighed to obtain their density. The compressive properties of these samples were investigated by studying the evolution of compressive stress as a function of compressive strain using an Instron 5944. Samples were compressed to a strain of 0.8 at 1 mm/min, followed by decompression at the same rate, to yield a stress-strain loop. Values of area within the curve, maximum stress, and compressive modulus obtained from these measurements have been reported.

Thermo-chemical Properties

The chemical composition of 75 samples was assessed by measuring the absorbance as a function of wave number (450 – 4000 cm^{-1}) on an ATR-FTIR setup (Perkin Elmer Spectrum 2). The plots have been shown between 450 – 2000 cm^{-1} since no noteworthy peaks were observed beyond this range. From the IR spectra, the absorbance values of the urea (1640 cm^{-1}) and urethane (1725 cm^{-1}) peaks were compared to obtain the urea : urethane ratio for every layer. Similarly, the MDI and TDI peaks were identified to be at 510 cm^{-1} and 454 cm^{-1} respectively.

The glass transition temperatures (T_g) of 45 samples were determined by performing DSC measurements on TA Instruments Discovery DSC 2500. Pre-weighed samples in a covered aluminum pan were subject to cyclic heating and cooling (10 C/min). The first heating cycle (30 °C to 130 °C) was performed to erase the thermal history of the sample, followed by a cooling cycle (130 °C to -80 °C) to impart known thermal history. A second heating ramp (-80 °C to 130 °C) was performed to obtain the T_g values. Thermal stability and degradation studies were performed (Perkin Elmer TGA 8000) on the foam layers.

Analytical Characterization

X-ray fluorescence (XRF) measurements were performed on a Rigaku ZSX Primus IV (WDXRF). Prior to measurement, the foam samples were densified by heating to 230 – 250 °C (resulting in a mass loss of 5–12 wt%), followed by compression under an applied load of 6 metric tons in a hydraulic press. Each sample was placed in a steel holder with an exposed circular section of diameter 1 cm and a measurement time of 13 minutes.

For PFAS detection, foam samples (2 of each type) were soaked in methanol, followed by sonication. The solvent samples were then characterized using a liquid chromatography setup coupled with a triple quadrupole mass spectrometry unit. The detection limit of this setup is typically in the sub-ppb ranges.

Thermogravimetric analysis, coupled with mass spectrometry (TGA-MS) measurements were performed by heating from room temperature to 230 °C at 10 °C / min, followed by an isothermal hold at 230 °C for 15 min. Prior to each measurement, the furnace was purged with nitrogen (25 mL/min) at room temperature for 15 mins to remove air, followed by equilibration at 50 °C. Mass spectra were obtained by analyzing evolved gases with molecular weights

between 1-200 amu. The maximum ion current at each molecular weight was determined and represented as a function of molecular weight (amu).

Microbial detection

Bacterial detection: Cubic foam samples (3 cm length) were gently stamped (5 out of 6 faces of the cube) of the sample on Brain Heart Infusion (BHI; Anaerobe Systems #AS-6426) and allowed to sit agar side down for 1 hour to ensure sufficient contact time with the final (sixth face) side; negative control included to confirm no plate contamination. The foam samples were then removed and incubated overnight at 37 °C, following which, the colonies were counted.

Mold detection: Cubic foam samples (3 cm length) were enclosed in Malt Extract Agar plates (Milllipore #146191) and allowed to sit (agar side down) for 1 hour to enable settling of mold spores on agar (settling plate method);[17] negative control included to confirm no plate contamination. The samples were then removed, and the plates were sealed with parafilm and stored in a closed drawer (agar side up) for up to 6 days at room temperature.

Figures

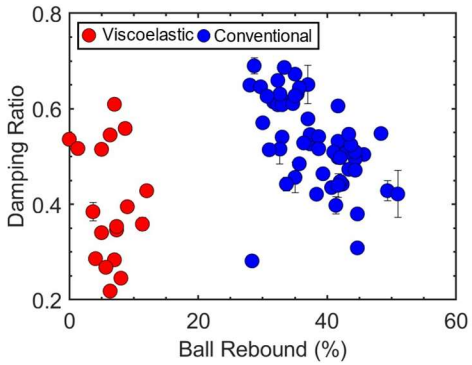

Figure A1: Damping ratio of viscoelastic and conventional foams as a function of rebound resilience.

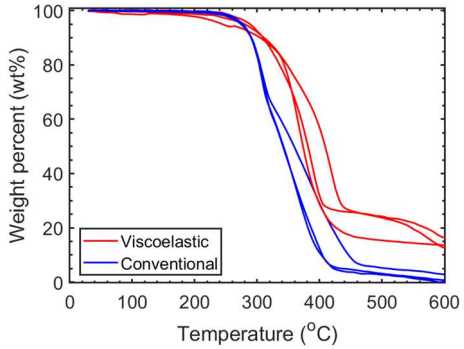

Figure A2: Thermogravimetric analysis (TGA) of viscoelastic and conventional foams (3 samples each). Minimal weight loss at temperatures < 250°C indicates the absence of VOCs. No significant differences in decomposition temperatures were noted between the two categories. A residual weight content was consistently observed for the viscoelastic foam layers.

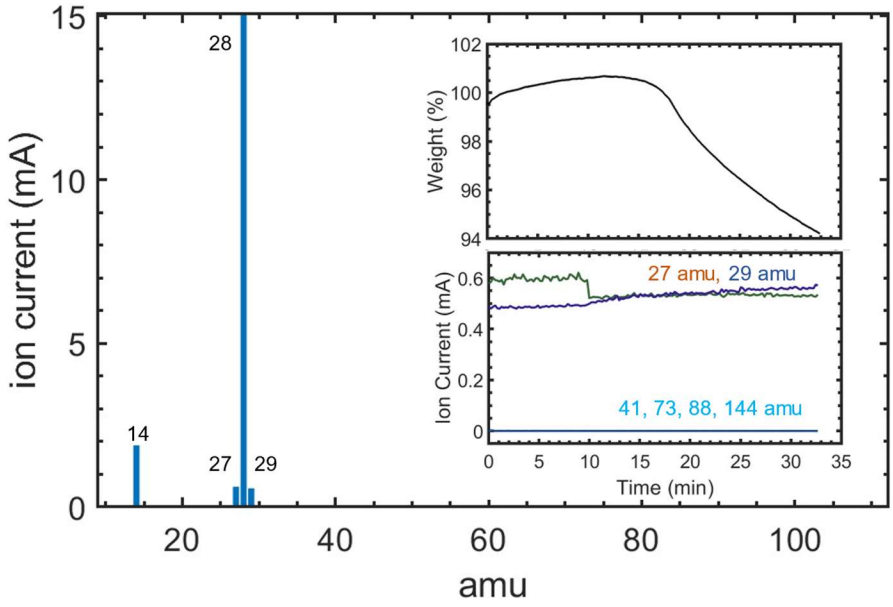

Figure A3: Mass spectrum of a representative conventional foam sample.

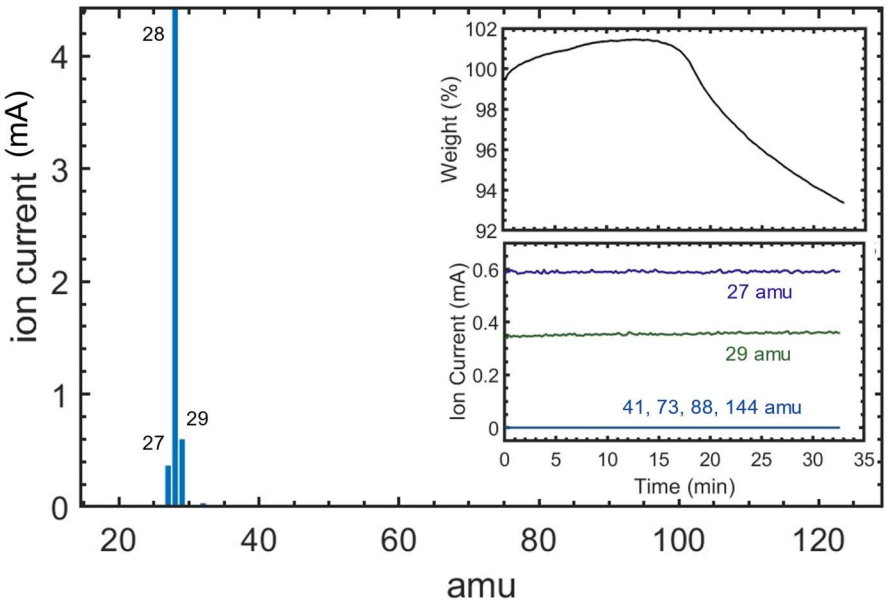

Figure A4: Mass spectrum of a representative conventional foam sample.

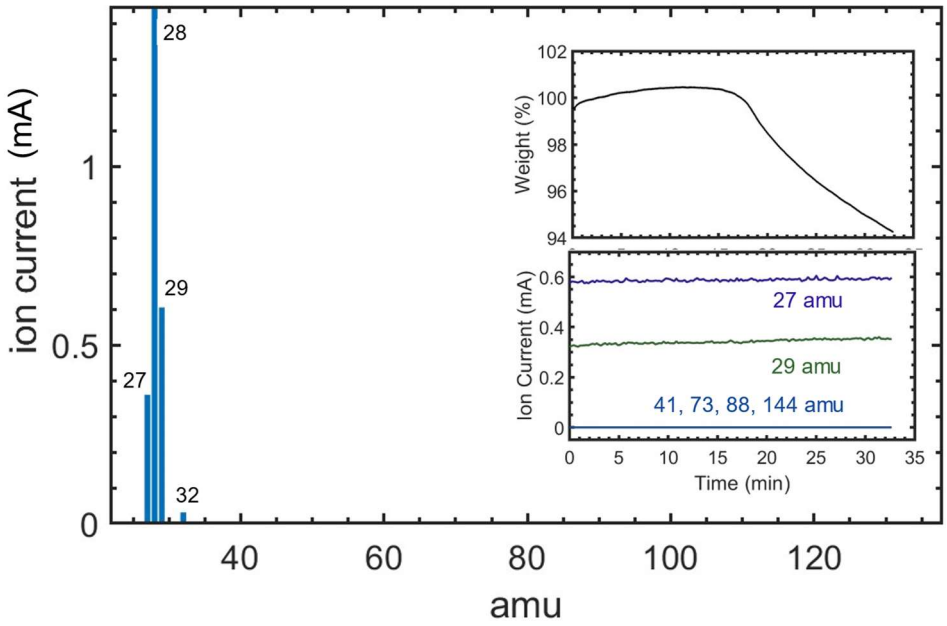

Figure A5: Mass spectrum of a representative conventional foam sample.

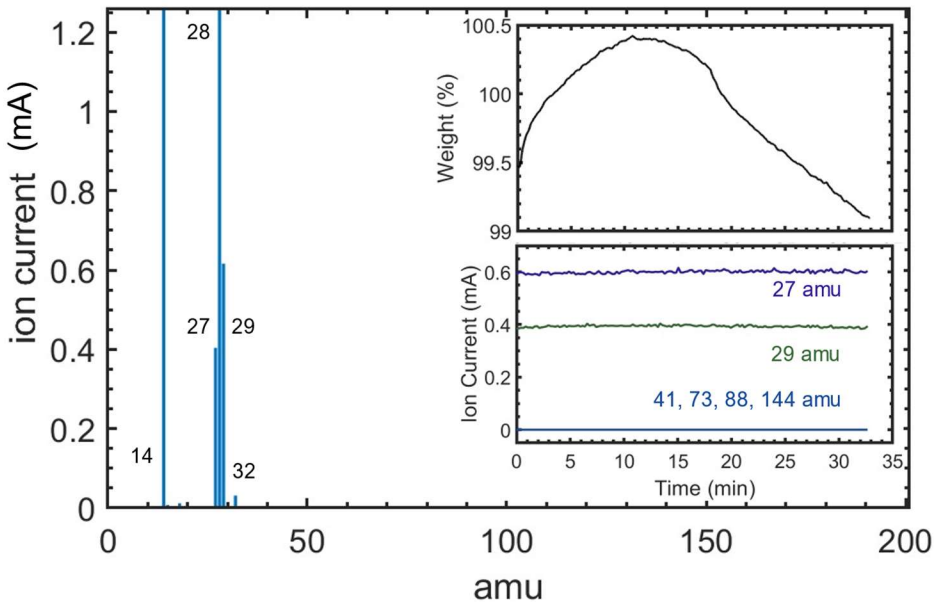

Figure A6: Mass spectrum of a representative viscoelastic foam sample.

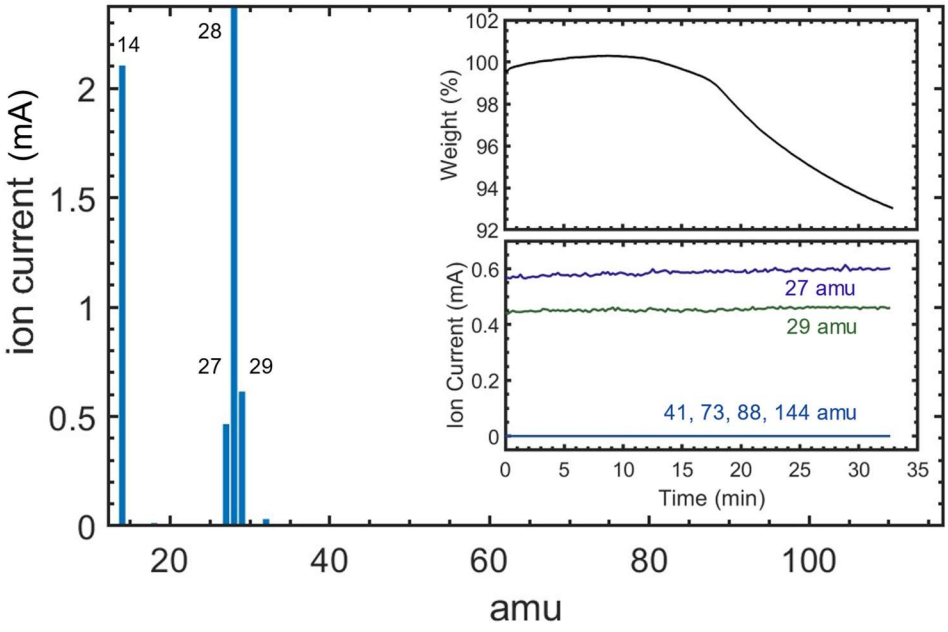

Figure A7: Mass spectrum of a representative viscoelastic foam sample.

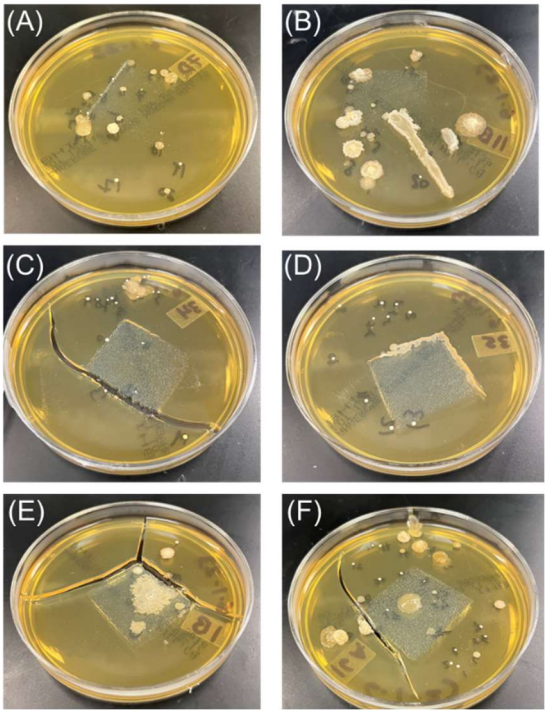

Figure A8: Proliferation of bacterial colonies in agar plates dabbed with **(A)–(B)** viscoelastic foam samples and **(C)–(F)** conventional samples.

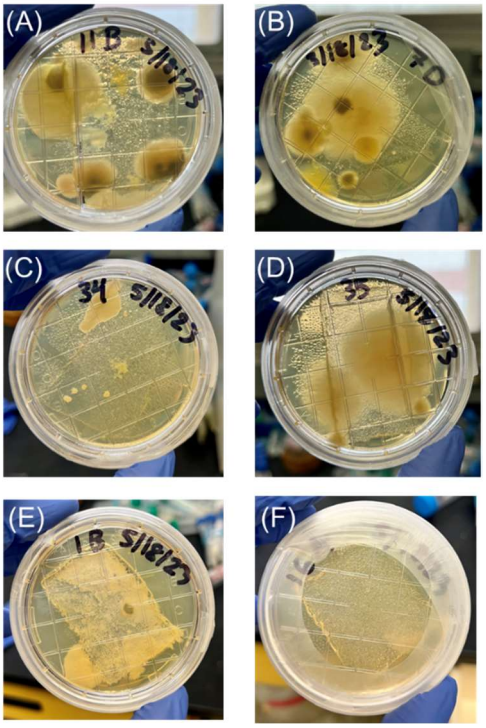

Figure A9: Proliferation of mold colonies in agar plates dabbed with **(A)–(B)** viscoelastic foam samples and **(C)–(F)** conventional samples.